ARCHIVES OF ELECTRICAL ENGINEERING VOL. 75(1), pp. 207–220 (2026)

DOI 10.24425/aee.2026.156809

Viscoelastic magnetic loss modeling in soft ferromagnetic materials using fractional derivatives

BENJAMIN DUCHARNE [1,2]✉

[1] *ELyTMaX IRL3757, CNRS, Univ Lyon, INSA Lyon, Centrale Lyon Université Claude Bernard Lyon 1, Tohoku University Sendai 980-8577, Japan*

[2] *LGEF, INSA-Lyon, UR682, University Lyon 69621 Villeurbanne, France*

e-mail: ✉ *benjamin.ducharne@insa-lyon.fr*

(Received: 15.11.2025, revised: 27.01.2026)

Abstract: Magnetization dynamics in soft ferromagnetic materials arise from the combined action of domain-wall motion and dissipative mechanisms linked to microscopic eddy currents and magnetic diffusion, leading to a viscoelastic-like behavior of the core losses. This work introduces a unified modeling framework based on fractional-derivative operators to capture these elastic and viscous contributions within a single constitutive law. Analytical expressions for dynamic losses under sinusoidal excitation are derived and validated using both literature data for classical ferromagnetic materials and new measurements on nanocrystalline 1K107A and 1K107B ribbons. The model achieves excellent accuracy, with NRMSE(%) values below 4%. A strong correlation (Pearson coefficient 0.93) is found between the dissipative parameter ρ and σd^2, suggesting a potentially universal relation. The results demonstrate that fractional viscoelastic modeling effectively describes magnetic losses and provides a powerful predictive tool for the design of high-efficiency magnetic components.

Key words: dynamic hysteresis, fractional derivative, macroscopic eddy currents, magnetic loss, microscopic eddy currents

1. Introduction

Magnetization processes are at the origin of a vast range of modern technologies, from power transformers and electric machines to inductors and high-frequency magnetic components. In such systems, magnetic losses remain a central limiting factor, as they directly impact energy

efficiency, thermal management, and long-term reliability. A precise understanding and accurate modeling of magnetization dynamics are therefore essential for both material development and device design [1–4].

From a modeling perspective, magnetic losses in soft ferromagnetic materials are traditionally interpreted through loss separation frameworks, most notably Bertotti's Statistical Theory of Losses (STL), which decomposes total losses into quasi-static hysteresis, classical eddy-current, and excess contributions [4]. This approach has proven extremely successful and remains the reference for engineering applications. However, although STL is firmly grounded in well-established theoretical developments, it relies on a decomposition of magnetic losses into distinct contributions governed by different physical assumptions. This structure limits its ability to provide a unified constitutive interpretation of magnetization dynamics, particularly in the presence of memory effects and non-integer power-law frequency dependencies.

In parallel, diffusion-based formulations derived from Maxwell's equations have been developed to account for macroscopic eddy currents and field inhomogeneities at higher frequencies [5, 6]. While these approaches correctly capture spatial effects, they do not explicitly describe the intrinsic viscoelastic nature of domain-wall dynamics and their coupling with dissipative mechanisms at the microscopic scale.

Recent experimental and theoretical studies have highlighted that magnetization dynamics in ferromagnetic alloys exhibit viscoelastic-like behavior, combining reversible (elastic) and dissipative (viscous) responses [7, 8]. This behavior originates from the coexistence of elastic domain-wall bulging within pinning potentials and rate-dependent damping associated with microscopic and macroscopic eddy currents. As a result, magnetic losses often follow power-law dependencies with frequency, suggesting the presence of long-term memory effects that are not naturally captured by classical integer-order models.

Fractional calculus has recently emerged as a powerful mathematical tool to describe such memory-dependent phenomena in viscoelastic systems. In the context of magnetism, fractional-derivative operators provide a compact way to interpolate between purely elastic and purely viscous responses, enabling a unified description of reversible and irreversible magnetization mechanisms [7, 9]. Several recent works have demonstrated the relevance of this approach for specific materials or excitation conditions; however, a systematic analytical formulation of magnetic losses and a clear physical interpretation of the associated parameters are still lacking.

The objective of the present work is to address this gap by proposing a unified viscoelastic framework for magnetic loss modeling based on fractional-derivative operators. The main contributions of this study are threefold. First, an analytical constitutive law is derived that links the dynamic magnetic field contribution directly to a fractional derivative of the magnetic flux density, leading to a closed-form expression for dynamic losses under sinusoidal excitation. Second, the proposed model is validated on a broad set of materials, including classical electrical steels and soft nanocrystalline ribbons, demonstrating excellent predictive accuracy over a wide frequency range. Third, a strong correlation is identified between the dissipative parameter ρ and the quantity σd^2, suggesting a potentially universal relation between electrical conductivity, sample thickness, and viscoelastic dissipation mechanisms.

By explicitly connecting magnetization dynamics, viscoelasticity, and fractional-order modeling, this work provides both a physical interpretation and a practical predictive tool for magnetic losses. The proposed framework complements existing loss separation approaches and offers new insights into the interplay between domain-wall kinetics, magnetic diffusion, and dissipative processes in soft ferromagnetic materials.

2. Magnetization process and viscoelasticity

2.1. Magnetization process

2.1.1. In the low-frequency range (quasi-static behavior)

At low excitation frequencies, the magnetization process can be considered quasi-static and the applied magnetic field remains spatially homogeneous. Under these conditions, the magnetization process involves a hierarchy of mechanisms with distinct energetic and dynamic characteristics, commonly described in standard textbooks [4,10]. At low magnetic field amplitudes, magnetization proceeds mainly through reversible and irreversible domain-wall motions (Fig. 1, [11, 12]). At higher magnetic fields, domain annihilation and coherent rotation progressively contribute to magnetization, enabling the material to approach saturation. These mechanisms involve shorter intrinsic time constants and higher activation energies (Figs. 1(a) and 1(b)).

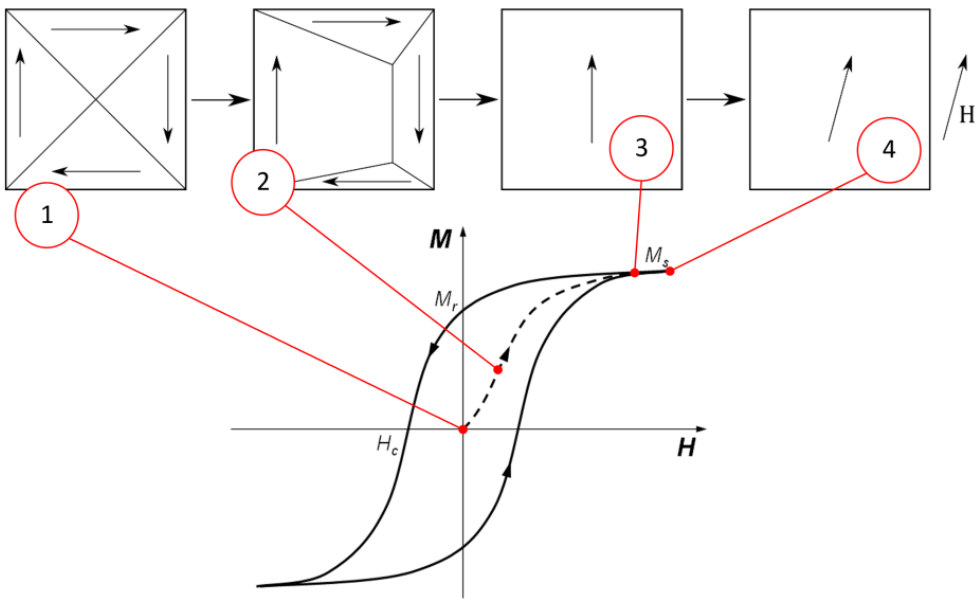

(a)

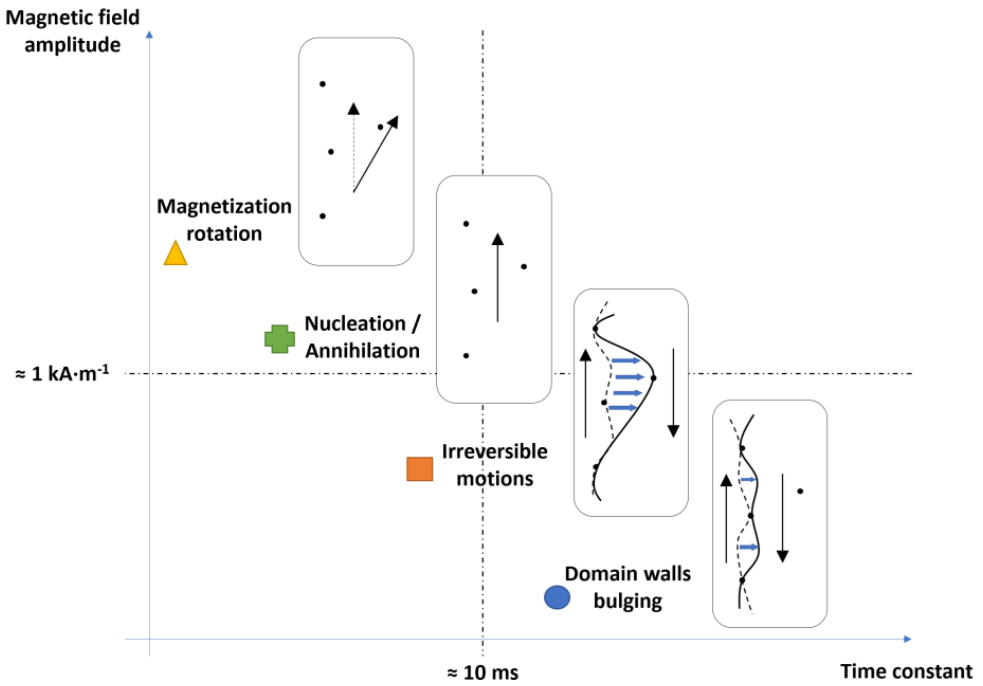

(b)

Fig. 1. Magnetization mechanisms, illustration graphic (a); magnetic field amplitude vs. time constant distribution of the magnetization mechanisms (b)

From a viscoelastic perspective, the key feature of the quasi-static regime is the coexistence of reversible (elastic-like) and irreversible (viscous-like) domain-wall processes. The reversible contribution stores magnetic energy and is fully recoverable, while the irreversible contribution leads to energy dissipation and defines the quasi-static hysteresis loss.

2.1.2. In the higher frequency range

When the excitation frequency increases, the magnetization process becomes progressively influenced by magnetic diffusion and macroscopic eddy currents, governed by Maxwell's equations [5, 13].

When the magnetic skin depth becomes comparable to the thickness, the magnetization process is no longer spatially homogeneous: regions close to the surface experience stronger and faster field variations, while inner regions respond with reduced amplitude and phase delay due to eddy-current shielding.

The widening of the hysteresis loop observed under increasing excitation frequency primarily results from the need to sustain a given magnetization rate against the growing eddy-current counterfield. This effect leads to an apparent increase in coercivity and dynamic losses, without invoking any enhancement of domain-wall mobility or displacement. On the contrary, eddy-current damping tends to restrict domain-wall motion by opposing rapid changes in magnetic flux.

From a viscoelastic standpoint, this regime corresponds to an increase in the effective viscous contribution of the magnetization process, as energy dissipation is dominated by rate-dependent losses associated with induced currents and delayed magnetic response. These effects introduce both temporal and spatial memory, which must be accounted for in predictive loss models.

2.2. Viscoelasticity

In the context of magnetization dynamics, the term "viscoelasticity" is used here in a constitutive and phenomenological sense, by analogy with mechanical systems [14, 15] that exhibit both energy storage and rate-dependent dissipation (see Fig. 2 for illustration).

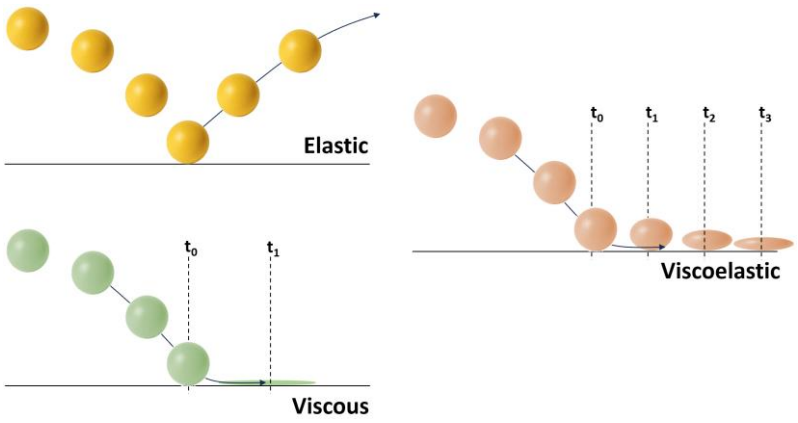

Fig. 2. Viscoelasticity: an illustration in a mechanical context

In soft ferromagnetic materials, reversible processes such as elastic domain-wall bulging contribute mainly to magnetic energy storage and to the phase relationship between magnetic field and flux density. Their contribution to magnetization reversal and energy dissipation remains minor, except at very low flux density amplitudes, where hysteresis losses are negligible. In contrast, irreversible processes, namely domain-wall depinning, excess losses, and eddy-current-induced damping-dominate the actual magnetization reversal and are responsible for the major part of magnetic losses.

The viscoelastic analogy therefore does not imply an equal contribution of elastic and viscous components, but rather reflects the coexistence of instantaneous (reversible) and rate-dependent (dissipative) responses in the magnetic constitutive behavior. From this perspective, the elastic-like contribution defines the quasi-static response, while the viscous-like contribution governs the frequency-dependent widening of the hysteresis loop and the associated power losses.

This interpretation is particularly useful for modeling purposes, as it allows magnetic losses to be expressed through constitutive laws that naturally incorporate memory effects and power-law frequency dependencies [16]. In the following section, this viscoelastic viewpoint is formalized using fractional-derivative operators, which provide a unified mathematical description of dominant dissipative mechanisms while retaining a minimal representation of reversible effects.

3. Fractional derivative as mathematical operator for the simulation of viscoelasticity

3.1. Fractional derivative: description

The fractional derivative is a mathematical extension of the classical concept of differentiation, in which the order of the derivative is not limited to integer values but can take any real or even complex value. In other words, while the first derivative represents the rate of change of a function and the second derivative represents the curvature, the fractional derivative of order n (with $0 < n < 1$, for example) describes a non-integer order of differentiation that lies between these two cases [17, 18]. This generalization allows for a more flexible and accurate description of systems that exhibit memory effects or non-local behavior, that is, systems whose present state depends not only on current conditions but also on their past history.

Unlike classical derivatives, which are defined locally (based solely on values of the function at a specific point), fractional derivatives are intrinsically non-local operators. They involve an integration over the past of the function, thereby introducing a natural mathematical framework for representing time-dependent phenomena where history plays a role. Several formulations of fractional derivatives exist, the most common being those of Riemann–Liouville, Caputo, and Grünwald–Letnikov, each differing slightly in how the historical weighting is treated but all sharing the same physical interpretation: a gradual transition between differentiation and integration.

Trigonometric functions are analytic, meaning they satisfy both the Laplace and Cauchy–Riemann equations [19]. This property enables the application of fractional calculus to describe their behavior under fractional differentiation, in other words, trigonometric functions admit analytical fractional derivative solutions:

$$\frac{\mathrm{d}^n}{\mathrm{d}t^n}\mathrm{e}^{i\omega t} = \omega^n \mathrm{e}^{i\left(\omega t + n\frac{\pi}{2}\right)}. \tag{1}$$

Fractional derivatives are particularly suitable for modeling viscoelastic systems, diffusion processes, and anomalous relaxation phenomena, where classical integer-order differential equations often fail to capture observed behaviors. In such systems, the fractional order n acts as a measure of memory, quantifying how strongly the past influences the present response. In the context of magnetization dynamics, fractional derivatives provide a powerful tool to describe the viscoelastic nature of the magnetization process, where elastic (instantaneous) and viscous (time-dependent) effects coexist.

3.2. Fractional derivative, viscoelasticity and core loss simulation

Under alternating magnetization conditions, the total magnetic energy losses W_{alt} in a ferromagnetic specimen can be decomposed into two main contributions:

$$W_{\mathrm{alt}} = W_{\mathrm{stat\,alt}} + W_{\mathrm{dyn\,alt}}, \tag{2}$$

where $W_{\mathrm{stat\,alt}}$ represents the frequency-independent quasi-static losses and $W_{\mathrm{dyn\,alt}}$ denotes the frequency-dependent dynamic losses [9].

The quasi-static losses $W_{\mathrm{stat\,alt}}$ are classically estimated from the area of the hysteresis loop $B_a(H_{\mathrm{surf}})$, where B_a is the magnetic flux density averaged across the specimen cross-section and

H_{surf} is the applied magnetic field:

$$W_{\text{stat alt}} = \int_0^{T_{\text{stat}}} \frac{\mathrm{d}B_a}{\mathrm{d}t} \cdot H_{\text{surf stat}} \mathrm{d}t \quad (\mathrm{J} \cdot \mathrm{m}^{-3}). \tag{3}$$

These losses mainly reflect domain wall motions occurring under slow magnetization changes.

The dynamic contribution $W_{\text{dyn alt}}$ arises when the material is subjected to faster field variations, limiting its ability to respond instantaneously. It includes both classical eddy-current losses, caused by macroscopic circulating currents, and excess losses, linked to the time-dependent rearrangement of magnetic domains.

Traditionally, these two effects are treated separately in Bertotti's Statistical Theory of Losses (STL [4,20,21]). However, using fractional derivative operators, they can be unified within a single analytical formulation. For a given sinusoidal magnetic flux density $B_a(t)$, the corresponding dynamic excitation field $H_{\text{surf}}(t)$ can be expressed as:

$$H_{\text{surf dyn}} = H_{\text{surf stat}} + H_{\text{dyn}} \quad (\mathrm{A} \cdot \mathrm{m}^{-1}), \tag{4}$$

where $H_{\text{dyn}}(t)$ accounts for time-dependent dissipation and is given by:

$$H_{\text{dyn}} = \rho \cdot \frac{\mathrm{d}^n B_a}{\mathrm{d}t^n} \quad (\mathrm{A} \cdot \mathrm{m}^{-1}). \tag{5}$$

Here, ρ is a material-dependent coefficient (with dimensions $\mathrm{A{\cdot}V^{-}}^{n}\mathrm{\cdot\ m}^{2n-1}$), and n the fractional order quantifies the degree of memory or time-dependence in the magnetization response.

This formulation draws a direct analogy with viscoelastic systems, where the stress–strain relationship is often described by a fractional differential equation to capture both instantaneous elastic response and time-dependent viscous flow. In magnetic materials, the elastic part corresponds to the reversible domain wall displacements, while the viscous damping is associated with the eddy currents (reversible and irreversible domain wall motions, macroscopic, etc.). The fractional operator naturally couples these two behaviors into a single constitutive law, thereby providing a viscoelastic interpretation of magnetic losses.

The resulting energy loss can then be written as:

$$W_{\text{dyn alt}} = \int_0^T \frac{\mathrm{d}B_a}{\mathrm{d}t} \cdot H_{\text{dyn}} \mathrm{d}t = \int_0^T \frac{\mathrm{d}B_a}{\mathrm{d}t} \cdot \rho \cdot \frac{\mathrm{d}^n B_a}{\mathrm{d}t^n} \mathrm{d}t \quad (\mathrm{J} \cdot \mathrm{m}^{-3}). \tag{6}$$

Assuming a sinusoidal magnetic flux density,

$$B_a = B_M \sin(\omega t) \quad (\mathrm{T}), \tag{7}$$

an analytical expression for the dynamic energy losses can be derived:

$$W_{\text{dyn alt}} = \rho \pi B_M^2 \omega^n \sin\left(n \frac{\pi}{2}\right) \quad (\mathrm{J} \cdot \mathrm{m}^{-3}). \tag{8}$$

This equation highlights the power-law dependence of magnetic losses on frequency, a hallmark of viscoelastic systems where energy dissipation scales with the rate of deformation. The fractional order n thus serves as a compact measure of the relative weight between reversible (elastic) and irreversible (viscous) magnetization mechanisms.

4. Experimental validation

To validate the simulation approach presented in Section 3.2, we first refer to the comparisons between simulation and experimental results previously discussed in [9], which concern a set of classical ferromagnetic materials. All material data (electrical conductivity, density and thickness) were taken from the scientific literature [22–25]. Together with the quantitative information associated with these comparisons, they are presented in Table 1.

Table 1. Experimental and simulation data for the first materials tested

Material	**Electrical conductivity σ**	**Density δ**	**Thickness d**	ρ	n	**NRMSE**
	($S \cdot m^{-1}$)	**($kg \cdot m^{-3}$)**	**(m)**	**($A \cdot V^{-n} \cdot m^{2n-1}$)**	**–**	**(%)**
FeCo [22]	$2.27 \cdot 10^6$	8 120	$0.201 \cdot 10^{-3}$	0.0275	0.885	2.19
NO FeSi [22]	$1.92 \cdot 10^6$	7 650	$0.194 \cdot 10^{-3}$	0.0805	0.793	1.63
GO FeSi [23]	$2.12 \cdot 10^6$	7 650	$0.27 \cdot 10^{-3}$	0.027	0.924	3.92
SMC [24]	$4.2 \cdot 10^4$	7 370	$3 \cdot 10^{-3}$	0.16	0.92	3.58
LC steel [25]	$1.99 \cdot 10^6$	7 850	$0.64 \cdot 10^{-3}$	0.22	1	1.06

Although reference [9] addressed both alternative and rotational magnetization, the present study is deliberately restricted to unidirectional (alternative) magnetization, which remains the most relevant configuration for the majority of practical applications. Identification of the model parameters was performed by fitting the analytical expression of the dynamic energy loss given in Eq. 8 to the experimentally measured loss values as a function of excitation frequency. For each material, the total energy loss per cycle was first determined from the measured hysteresis loops using Eq. 6. When necessary, the quasi-static contribution was subtracted so that only the dynamic loss component $W_{\mathrm{dyn\,alt}}$ was considered.

The parameters ρ and n were then identified by minimizing the Normalized Root Mean Square Error (NRMSE), expressed in %, as described in Eq. 9 between measured and simulated losses over the investigated frequency range. The fitting was carried out using a nonlinear least-squares procedure, with ρ and n treated as frequency-independent material parameters:

$$\mathrm{NRMSE}\,(\%) = 100 \frac{\sqrt{\dfrac{1}{N}\displaystyle\sum_{i=1}^{N}\left(W_{\mathrm{sim}_i} - W_{\mathrm{meas}_i}\right)^2}}{\max\left(W_{\mathrm{meas}_i}\right)}. \tag{9}$$

Figure 3 shows the simulation-measurement comparisons for most of the materials listed in Table 1. The LC steel was excluded because the amount of available experimental data was too limited. For all tested materials, the NRMSE(%) remained below 4%.

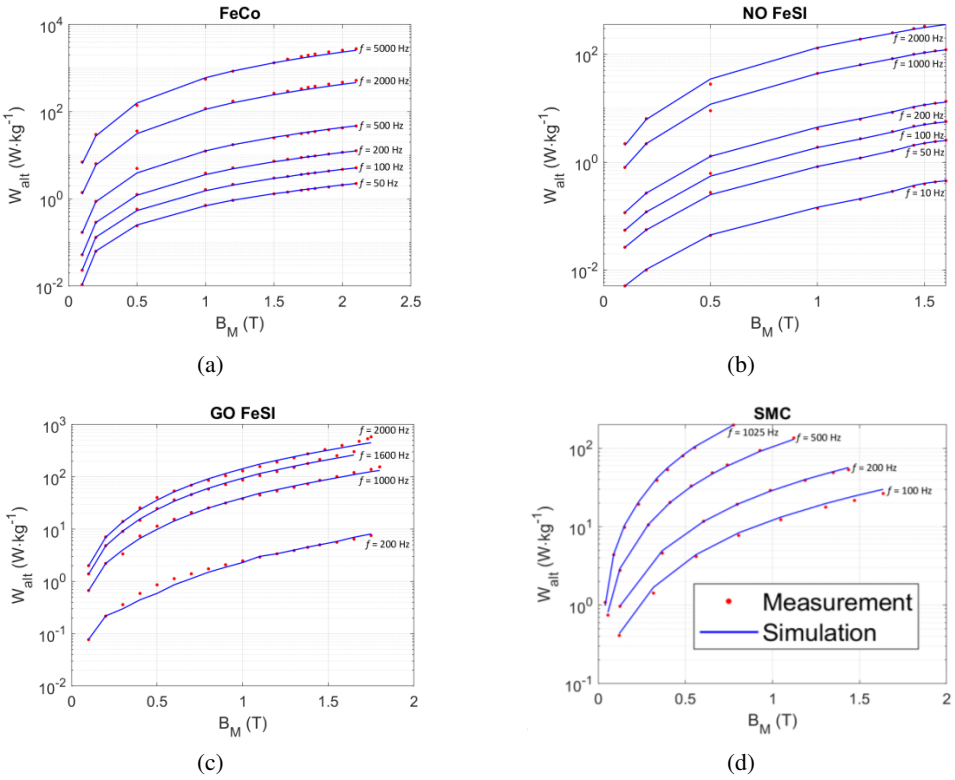

Fig. 3. Comparison between simulation and measurement under alternating undirectional magnetization for four classical ferromagnetic materials: FeCo (a); NO FeSi (b); GO FeSi (c); SMC (d)

All materials listed in Table 1 are well-established ferromagnetic materials commonly used in practical applications. However, to further challenge the proposed simulation approach, we sought to evaluate it on an alternative material with a markedly different microstructural and magnetic behavior.

To complement this initial assessment of the simulation accuracy, in the next section the method was therefore applied to a typical soft nanocrystalline alloys, selected as a representative modern ferromagnetic material widely recommended for power electronic applications. These alloys exhibit very low coercivity, high permeability, and well-defined magnetization mechanisms, making it an appropriate candidate for assessing the predictive capability of the fractional-derivative formulation.

4.1. Experimental setup and tested specimen

4.1.1. Description of the experimental setup

An experimental setup was developed to record hysteresis loops under varying magnetic field amplitudes and excitation frequencies. In accordance with international standards [26, 27], the system operated under sinusoidal magnetic flux density control. Both the excitation and sensing coils were wound with five turns each. The measurements were carried out using a Brockhaus HG 200 AC hysteresisgraph (Brockhaus Group, Lüdenscheid, Germany) configured for sinusoidal polarization.

In this configuration, the system operates under a closed-loop B_a-control: the instrument continuously monitors the induced secondary (search-coil) voltage, proportional to $\mathrm{d}B_a/\mathrm{d}t$, and adjusts the magnetizing drive via the power amplifier to ensure that the flux density B_a follows a sinusoidal setpoint. This feedback mechanism, implemented through a PID-type control algorithm, maintains the sinusoidal waveform of B_a even at high frequencies.

The experimental setup included a signal generator, a power amplifier, and a feedback control system, enabling excitation frequencies from up to 100 kHz. Because the power supply could not sustain ideal DC conditions, measurements obtained at 10 Hz were treated as quasi-static hysteresis loops. The conversion of raw data into $B_a(H_{\mathrm{surf}})$ curves followed standard procedures: the surface magnetic field H_{surf} was calculated from the magnetizing current and the geometry of the magnetic circuit, while the flux density B_a was derived from the time integral of the induced voltage in the search coil. The resulting $B_a(H_{\mathrm{surf}})$ loops were then reconstructed from the instantaneous values of B_a and H_{surf} over a full magnetization cycle and the core loss calculated from Eq. 10 below:

$$W_{\mathrm{alt}} = \int_0^T \frac{\mathrm{d}B_a}{\mathrm{d}t} \cdot H_{\mathrm{surf}}\,\mathrm{d}t \quad (\mathrm{J}\cdot\mathrm{m}^{-3}). \tag{10}$$

Above $f = 100$ kHz and high B_a, maintaining a perfectly sinusoidal flux density would require current transients of excessively high amplitude, exceeding the amplifier capabilities and distorting the control signal, thereby defining the upper frequency limit of the setup.

4.1.2. Description of the tested nanocrystalline specimens

The nanocrystalline specimens investigated in this study consist of two Fe-based nanocrystalline ribbons, 1K107A and 1K107B, supplied by Junda Company (Hefei, China). These materials are specifically designed for high-frequency magnetic applications, such as common-mode chokes, power transformers, current sensors, and magnetic shielding. In order to ensure that the conclusions drawn in this work are representative of nanocrystalline materials used in industrial practice, both ribbons were tested in the form of commercially relevant toroidal cores with substantial magnetic volume.

The two grades share a very similar alloy composition and nanocrystalline microstructure, but they differ slightly in processing route, which may affect their high-frequency loss behavior. In particular, 1K107B is typically optimized for thinner ribbon configurations and improved high-frequency performance, whereas 1K107A represents a more standard nanocrystalline ribbon grade.

For both materials, the ribbon thickness was $d = 25$ µm, the mass density $\delta = 7180$ kg·m^3, and the electrical conductivity $\sigma = 0.8 \cdot 10^6$ S·m^2. The ring-shaped cores had an inner diameter of 50 mm and an outer diameter of 80 mm, corresponding to a mean magnetic path length of $l = 0.2$ m and a cross-sectional area of $A = 3.75 \cdot 10^{-4}$ m^2.

The magnetic properties of nanocrystalline ribbons depend critically on the annealing process, which governs the formation of ultrafine grains (10–20 nm) within the amorphous matrix. Proper annealing enhances the soft magnetic characteristics, whereas deviations from optimal conditions can cause grain growth and increased hysteresis losses.

In everyday applications, nanocrystalline ferromagnetic materials are typically used in the frequency range of $f = 10$ kHz to several hundred kHz, where their low core losses and high permeability make them ideal for high-efficiency and compact magnetic components. Even at

f = 100 kHz, the calculated skin depth remains larger than half the ribbon thickness. As a result, macroscopic eddy currents can be considered reduced, and the magnetic field distribution across the ribbon can be assumed relatively homogeneous in the simulation methods described in this study.

4.2. Comparison between simulation and measurement for the 1K107A and the 1K107B nanocrystalline ribbon and discussions

Based on their very limited coercivity in the quasi-static range (< 5 A·m^{-1}), no static contribution ($W_{\text{stat alt}} = 0$) was considered for the simulation of the nanocrystalline ribbons losses. Figure 4 shows the simulation-measurement comparisons and Table 2 provides the simulation data used to obtain the best fit. Excellent NRMSE(%) of 2.66 and 0.95 were obtained confirming the good adaptability of the viscoelastic simulation method to very different kind of ferromagnetic materials.

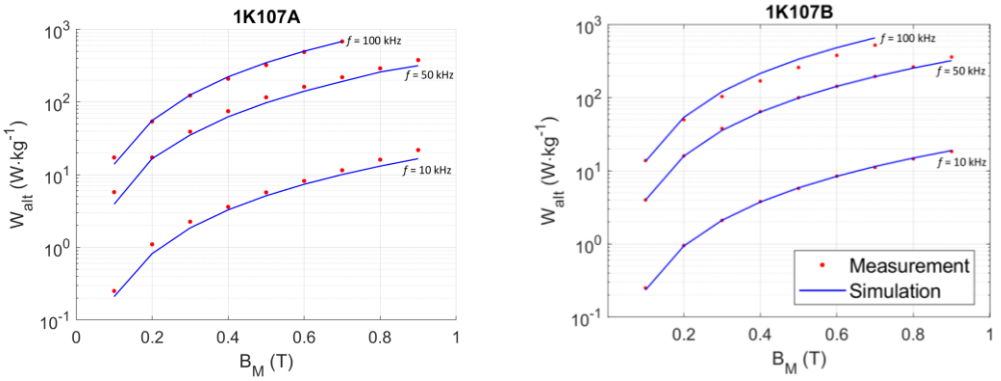

(a) (b)

Fig. 4. Comparison of the magnetic power loss between simulation and measurement under alternating undirectional magnetization for the 1K107A (a) and the 1K107B (b) nanocrystalline materials

Table 2. Experimental and simulation data for the 1K107A and 1K107B

Material	**Electrical conductivity σ**	**Density δ**	**Thickness d**	**ρ**	**n**	**NRMSE**
	(S·m^{-1})	**(kg·m^{-3})**	**(m)**	**(A·V^{-n}·m^{2n-1})**	**–**	**(%)**
1K107A	$0.8 \cdot 10^6$	7 180	$25 \cdot 10^{-6}$	$4.96 \cdot 10^{-4}$	0.832	2.66
1K107B	$0.8 \cdot 10^6$	7 180	$25 \cdot 10^{-6}$	$1.3 \cdot 10^{-3}$	0.76	0.95

A detailed analysis of the simulation data reported in Tables 1 and 2 reveals the following:

– The nanocrystalline ribbons 1K107A and 1K107B exhibit the lowest values of the fractional derivative order n, with n = 0.832 for 1K107A and n = 0.76 for 1K107B. These low values indicate a strong elastic contribution in the dynamic magnetization process compared to conventional soft magnetic materials. Nevertheless, for all tested materials, n remains close to unity,

indicating that the overall dynamic response still lies near that of a viscous regime, thereby confirming the dominant role of dissipative processes in the thermodynamic exchanges.

– The parameter ρ exhibits significantly larger variations across the different material classes. Although its numerical value differs between 1K107A ($\rho = 4.96 \cdot 10^{-4}$) and 1K107B ($\rho = 1.3 \cdot 10^{-3}$), both values remain of the same order of magnitude and are markedly lower than those identified for conventional electrical steels. From a relative standpoint, the two nanocrystalline ribbons therefore form a consistent group, despite the apparent quantitative difference when considered in isolation.
– As initially proposed in [9], a linear relationship between ρ and the parameter σd^2 (where σ is the electrical conductivity and d the ribbon thickness) was identified using a minimization of the relative Euclidean distance. By including the additional results obtained for the 1K107B nanocrystalline ribbon, this relationship has been slightly updated and is now expressed as:

$$\rho = 0.2715\sigma d^2 + 0.0152. \tag{11}$$

The updated linear fit yields a Pearson correlation coefficient of $r = 0.93$, demonstrating that the inclusion of the second nanocrystalline ribbon does not alter the validity of the relationship but rather reinforces its robustness across different material classes, including nanocrystalline alloys.

In Fig. 5, the values of ρ obtained for the nanocrystalline 1K107A and 1K107B cores are represented by a single point, denoted ρ_{Nano} in the legend, since their values remain very close when compared to those of the other investigated materials.

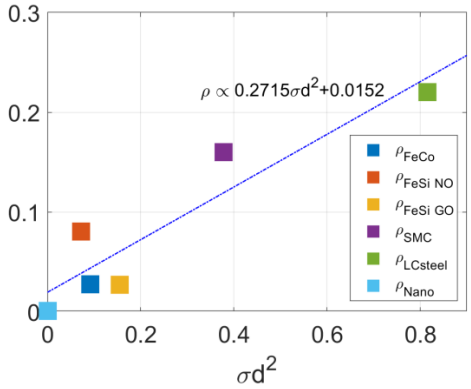

Fig. 5. ρ vs. σd^2 and linear fit for all tested materials

5. Conclusions

This work provides a unified physical and mathematical framework for describing core losses in soft ferromagnetic materials by interpreting magnetization dynamics through a viscoelastic perspective. By linking the reversible (elastic) and irreversible (viscous) components of the magnetization process to fractional-order differential operators, the proposed model captures both the instantaneous and time-dependent responses of magnetic domains over a wide frequency range.

The fractional-derivative formulation enables the dynamic magnetic field contribution to be expressed in a compact analytical form that naturally accounts for microscopic eddy currents, excess losses, and the intrinsic memory effects of ferromagnetic materials. The resulting loss expression, governed by two material parameters (ρ and n), provides an accurate power-law dependency with respect to frequency, consistent with experimental observations.

Extensive validation was performed using classical ferromagnetic materials from the literature, followed by experiments on soft nanocrystalline 1K107A and 1K107B cores. In all cases, the model reproduced the measured energy losses with excellent accuracy, with NRMSE(%) values consistently below 4%. Notably, the nanocrystalline ribbons exhibited the lowest fractional orders n, reflecting their higher elastic contribution and confirming the predominance of dissipative, viscous-like behavior across all tested materials. Furthermore, the updated linear relation between ρ and σd^2, supported by a high Pearson correlation coefficient (0.93), suggests a potentially universal link between electrical conductivity, ribbon thickness, and viscoelastic dissipation.

Overall, the results demonstrate that the viscoelastic interpretation of magnetization dynamics, combined with fractional-derivative modeling, provides a powerful and generalizable approach for predicting core losses under alternating excitation. This framework offers new insights into the interplay between magnetic diffusion, domain-wall kinetics, and dissipative mechanisms, and paves the way for improved material characterization and optimized magnetic component design in modern power electronics.

References

[1] Vukosavic S.N., *Electrical machines*, Springer Science & Business Media (2012).

[2] Lei G., Zhu J., Guo Y., Liu C., Ma B., *A review of design optimization methods for electrical machines*, Energies, vol. 10, no. 12, 1962 (2017), DOI: 10.3390/en10121962.

[3] Goodenough J.B., *Summary of losses in magnetic materials*, IEEE Transactions on Magnetics, vol. 38, no. 5, pp. 3398–3408 (2002), DOI: 10.1109/TMAG.2002.802741.

[4] Bertotti G., *Hysteresis in magnetism: for physicists, materials scientists, and engineers*, Academic Press (1998).

[5] Raulet M.A., Ducharne B., Masson J.P., Bayada G., *The magnetic field diffusion equation including dynamic hysteresis: a linear formulation of the problem*, IEEE transactions on magnetics, vol. 40, no. 2, pp. 872–875 (2004), DOI: 10.1109/TMAG.2004.824816.

[6] Maloberti O., Meunier G., Lebouc A.K., *Hysteresis of soft materials inside formulations: Delayed diffusion equations, fields coupling, and nonlinear properties*, IEEE Transactions on Magnetics, vol. 44, no. 6, pp. 914–917 (2008), DOI: 10.1109/TMAG.2007.915888.

[7] Ducharne B., Sebald G., *Fractional derivatives for the core losses prediction: State of the art and beyond*, Journal of Magnetism and Magnetic Materials, vol. 563, 169961 (2022), DOI: 10.1016/j.jmmm.2022.169961.

[8] Gao S., Ducharne B., Gao Y., Zhao X., *Simulation Strategies for Magnetic Losses in Electrical Steel Under PWM-Type Conversions: Two Models Comparison*, IEEE Transactions on Industry Applications (2025), DOI: 10.1109/TIA.2025.3574057.

[9] Ducharne B., Sebald G., *Analytical expressions of the dynamic magnetic power loss under alternating or rotating magnetic field*, Mathematics and Computers in Simulation, vol. 229, pp. 340–349 (2025), DOI: 10.1016/j.matcom.2024.10.009.

[10] Amano E., Valenzuela R., Irvine J.T., West A.R., *Domain wall relaxation in amorphous ribbons*, Journal of Applied Physics, vol. 67, no. 9, pp. 5589–5591 (1990), DOI: 10.1063/1.345893.

[11] Cizeau P., Zapperi S., Durin G., Stanley H.E., *Dynamics of a ferromagnetic domain wall and the Barkhausen effect*, Physical Review Letters, vol. 79, no. 23, 4669 (1997), DOI: 10.1103/PhysRevLett.79.4669.

[12] Fagan P., Zhang S., Sebald G., Uchimoto T., Ducharne B., *Barkhausen noise hysteresis cycle: Theoretical and experimental understanding*, Journal of Magnetism and Magnetic Materials, vol. 578, 170810 (2023), DOI:10.1016/j.jmmm.2023.170810.

[13] Huray P.G., *Maxwell's equations*, John Wiley & Sons (2009).

[14] Phan-Thien N., Mai-Duy N., *Understanding viscoelasticity: an introduction to rheology*, Berlin: Springer (2013).

[15] Banks H.T., Hu S., Kenz Z.R., *A brief review of elasticity and viscoelasticity for solids*, Advances in Applied Mathematics and Mechanics, vol. 3, no. 1, pp. 1–51 (2011), DOI: 10.4208/aamm.10-m1030.

[16] Ducharne B., Gao S., Gao Y., Zhao X., *Viscoelastic modeling of magnetic losses in a nanocrystalline core using fractional derivative operators*, Nonlinear Dynamics, vol. 2, pp. 1–6 (2025), DOI: 10.1007/s11071-025-11226-9.

[17] Kiryakova V.S., *Generalized fractional calculus and applications*, CRC press (1993).

[18] Petras I., *Fractional calculus and its applications*, Mathematical Modeling with Multidisciplinary Applications, pp. 355–396 (2012).

[19] Stein E.M., Shakarchi R., *Complex analysis*, vol. 2, Princeton University Press (2010).

[20] Chwastek K., Najgebauer M., Koprivica B., Divac S., Rosić M., *Two Approaches to Model Power Loss Under Increased Excitation Frequency*, Acta Physica Polonica: A, vol. 146, no. 1 (2024), DOI: 10.12693/APhysPolA.146.9.

[21] Ragusa C., Zhao H., Appino C., Khan M., de la Barrière O., Fiorillo F., *Loss decomposition in non-oriented steel sheets: The role of the classical losses*, IEEE Magnetics Letters, vol. 7, pp. 1–5 (2016), DOI: 10.1109/LMAG.2016.2604204.

[22] Appino C., de La Barrière O., Beatrice C., Fiorillo F., Ragusa C., *Rotational magnetic losses in nonoriented Fe–Si and Fe–Co laminations up to the kilohertz range*, IEEE Transactions on Magnetics, vol. 50, no. 11, pp. 1–4 (2014), DOI: 10.1109/TMAG.2014.2325968.

[23] Li Y., Zhu J., Yang Q., Lin Z.W., Guo Y., Zhang C., *Study on rotational hysteresis and core loss under three-dimensional magnetization*, IEEE Transactions on Magnetics, vol. 47, no. 10, pp. 3520–3523 (2011), DOI: 10.1109/TMAG.2011.2153186.

[24] Perigo E.A., Weidenfeller B., Kollár P., Füzer J., *Past, present, and future of soft magnetic composites*, Applied Physics Reviews, vol. 5, no. 3 (2018), DOI: 10.1063/1.5027045.

[25] Fiorillo F., *Characterization and measurement of magnetic materials*, Academic Press (2004).

[26] Fagan P., Ducharne B., Zurek S., Domenjoud M., Skarlatos A., Daniel L., Reboud C., *Iterative methods for waveform control in magnetic measurement systems*, IEEE Transactions on Instrumentation and Measurement, vol. 71, pp. 1–13 (2022), DOI: 10.1109/TIM.2022.3199198.

[27] IEC 60404-6, *Magnetic materials – Part 6: Methods of measurement of the magnetic properties of magnetically soft metallic and powder materials at frequencies in the range 20 Hz to 100 kHz by the use of ring specimens*, International Electrotechnical Commission (2010).